Nanowire Synthesis

DOI: 10.1002/ange.200801162

Synthesis of Lead Chalcogenide Alloy and Core–Shell Nanowires**

*Taleb Mokari, Susan E. Habas, Minjuan Zhang, and Peidong Yang**

Control over the dimensions and shape of nanostructures represents one of the main challenges in modern materials science. Morphology control of a variety of materials can be achieved using vapor–liquid–solid[1,2] or solution–liquid–solid techniques[3] to obtain one-dimensional (1D) systems. The unique optical and electrical properties of 1D nanostructures make them one of most important building blocks for nanoscience and nanotechnology applications, and provide the opportunity for their integration in electronic, photonic,[4] thermoelectric, and sensor-based devices.[5]

Size control has been traditionally important and necessary to tune the optical and electrical properties of nanomaterials by changing the band gap. This is particularly important in the strong confinement region, where one of the dimensions is smaller than the corresponding excitonic Bohr diameter.[6] Semiconductor alloy and core–shell nanowire systems represent another interesting direction towards functional nanostructures with enhanced structural and property tunability.

Herein, we focus on preparing novel 1D heterostructures of IV–VI semiconductor nanomaterials. Lead chalcogenides are known to be good materials for thermoelectrics due to their low thermoconductivity. Pseudobinary (e.g. PbSeTe) and pseudoternary alloys (e.g. PbSnSeTe) have even lower lattice thermal conductivities than the binary compounds due to disorder-induced phonon scattering processes. Lead chalcogenide materials are also good candidates for multi-exciton-generation (MEG) solar cells.[7] For example, previous reports showed quantum efficiencies as high as 300% and 700% for PbSe nanoparticles.[8,9]

Heterostructured alloy and core–shell nanomaterials have previously been shown for various materials, mainly II–VI semiconductor nanocrystals. For example, a quasi 1D system of CdSe–ZnS has been reported,[10] other systems include PbSe–PbS core–shell and alloy spherical nanoparticles developed by Lifshitz and co-workers.[11,12] In addition, Talapin et al. have demonstrated the growth of PbS and Au onto PbSe nanowires.[13] The physical properties of these heterostructured nanosystems are of interest for various applications as shown by the electronic structure calculations carried out by different groups.[14,15]

[*] Dr. T. Mokari, S. E. Habas, Prof. P. Yang
Department of Chemistry, University of California
Berkeley, CA 94720 (USA)
Fax: (+1) 510-642-7301
E-mail: p_yang@berkeley.edu
Dr. M. Zhang
Materials Research Department, Toyota Technical Center
Toyota Motor Engineering & Manufacturing North America (USA)

[**] T.M. thanks the Fulbright Foundation for a postdoctoral fellowship.

Here we demonstrate the formation of lead chalcogenide heterostructure nanowires by a solution-phase synthesis at moderate temperatures (see the Experimental Section). Two types of heterostructures (alloy and core–shell) were prepared by changing the concentration and temperature of the reaction. We were able to control the composition of the alloy and the thickness of the shell by changing the growth parameters. Three different systems, $PbSe_xS_{1-x}$ alloys, and PbSe–PbS and PbSe–PbTe core–shell nanowires were prepared. Achieving these three targeted structures is nontrivial due to various competitive processes such as ripening and formation of pure PbS (PbTe) nanoparticles.

The synthesis of PbSe nanowires is based on a previous report by Murray and co-workers.[16] The same procedure was used to prepare the PbSe nanowires used here as templates for further growth to give the alloy and core–shell nanostructures. The diameter of the core nanowires could be controlled and varied from 4 nm up to 100 nm, with a length of a few tens of micrometers.

The PbSe nanowires (Figure 1A) were used as templates to form $PbSe_xS_{1-x}$ alloy wires. Figure 1B shows $PbSe_{0.4}S_{0.6}$ alloy nanowires that were prepared by the slow addition of Pb and S precursors to a hot solution containing PbSe nanowires. (a detailed description of the synthesis can be found in the Experimental Section). The diameter of the alloy nanowires increased from 6 nm (pure PbSe nanowires) to ca. 10 nm, indicating the incorporation of additional material into the nanowires.

Structural characterization of the alloy system was carried out using various methods as shown in Figure 1. Figure 1D shows a high-resolution transmission electron microscopy (HRTEM) image of the $PbSe_{0.4}S_{0.6}$ nanowires. The lattice-resolved image indicates that the nanowires are growing along the ⟨100⟩ direction. X-ray diffraction (XRD) measurements of the alloy nanowires are shown in Figure 1C. The pattern can be indexed to a structure intermediate between the cubic PbSe and cubic PbS bulk phases, which strongly supports the formation of an alloyed structure. An energy-dispersive X-ray (EDX) spectrum (Figure 1E) taken on a small area of the alloy nanowire, shown in Figure 1D, indicates the presence of Se from the original PbSe nanowires, Pb from the original and added materials, and Cu from the TEM grid. However, due to overlap between the Pb and S peaks, electron energy loss spectroscopy (EELS) was necessary to detect the incorporation of S. The energy loss peak for S was observed at 165 eV (Figure 1F), providing clear evidence for the existence of S in the alloy nanowires. The EDX and EELS spectra were taken from the same area of the nanowire shown in Figure 1D. Tuning the alloy composition can be achieved by simply controlling the reaction conditions. For example, altering the S concentration will act to tune the alloy composition. The actual composition was determined by

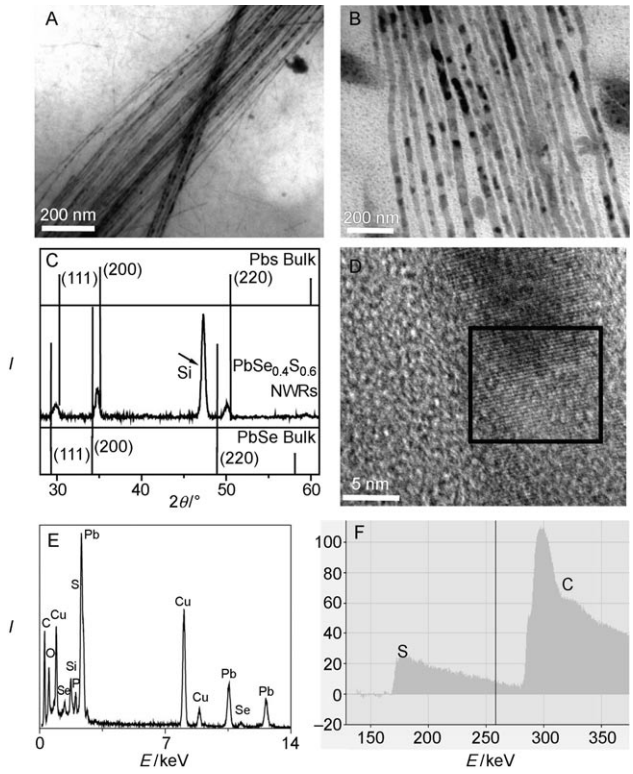

Figure 1. Structural characterization of $PbSe_{0.4}S_{0.6}$ core–shell nanowires. A) PbSe nanowires before PbS addition, B) the resulting $PbSe_{0.4}S_{0.6}$ alloy nanowires, C) powder XRD pattern of PbSeS alloy nanowires, D) HRTEM image of a single nanowire, E) EDX spectrum taken from the selected area denoted by a black square shown in (D), and F) an EELS spectrum of the same area.

measuring the ratio between the Pb and the Se in the EDS spectrum, and correlating it to the (200) peak shift in the XRD pattern

We suggest two possible mechanisms for the formation of the alloy materials. The first possible mechanism starts with a ripening process of the PbSe nanowires followed by growth of the $PbSe_xS_{1-x}$ alloy, while the second mechanism is based on a diffusion process between the PbSe core and a PbS shell. In the first mechanism, a ripening process promotes the dissolution of the PbSe nanowires, releasing Pb and Se precursors into solution, which, along with the added Pb and S precursors, can form alloyed materials. The second proposed mechanism can be divided into two stages. Initially, addition of the Pb and S precursors to the PbSe nanowires in solution results in the growth of PbS as a shell. In the second stage, the high temperature and the small diameter of the PbSe core encourage diffusion between the core and shell as an energetically favorable process to form the alloy. The high temperature was a critical factor necessary to obtain an alloy and not a shell. The second important factor is the diameter of the PbSe nanowires, with smaller diameters being more reactive and less energetically stable. The third factor is that the lattice mismatch between the core and the shell is not large ($a_{PbSe}/a_{PbS} = 3\%$ and $a_{PbSe}/a_{PbTe} = 5\%$; where a is the lattice constant of the crystals), which makes alloy formation more favorable.

A control experiment that was carried out under the same conditions without the addition of Pb and S precursors suggests that the first mechanism is more likely. The PbSe nanowires passed through the same ripening process in the absence of Pb and S precursors, resulting in a change in diameter from 6 nm (before heating) to ca. 7.5 nm (after heating at 190 °C). The increase in diameter is smaller (in the control) than that observed for the alloy, which indicates that there is a reaction between the PbSe and the Pb and S precursors leading to the formation of larger diameter wires.

The successive ion layer adsorption and reaction (SILAR) technique is a successful approach for growing a conformal shell over template materials with nanoscale dimensions. Ideally, growth of the shell occurs one monolayer at a time, by alternating addition of cationic and anionic precursors to the reaction mixture containing PbSe core nanowires (see the Experimental Section). The growth of the shell occurred at 130 °C, a temperature much lower than that required for alloy formation. Changing the concentration of the precursors allowed for control of the shell thickness. For example, increasing the concentration of S from 2 mM to 4 mM changed the coverage from four monolayers to six monolayers (for 30 mg of PbSe nanowires in both cases). The SILAR approach has two main advantages over the continuous addition of both precursors: 1) Inhibiting the formation of PbS nanoparticles at high temperature and, 2) preventing formation of the alloy materials. Using SILAR, homogeneous nucleation of PbS nanoparticles in solution is excluded because Pb and S are not present in the growth solution at the same time. Growth of the shell begins with adsorption of Pb on the surface of the nanowires, with the secondary addition of S providing a monolayer of PbS as conformal shell.

Structural characterization of the PbSe–PbS core–shell nanowires is shown in Figure 2. The diameter of the nanowires increased from 6 nm to ca. 11 nm following growth of

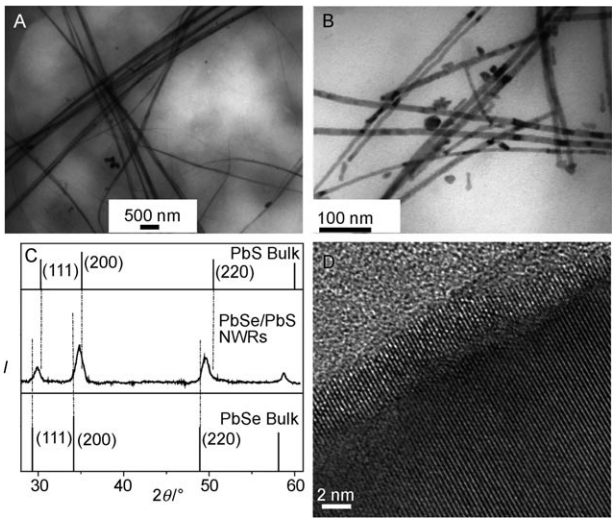

Figure 2. Structural characterization of PbSe–PbS core–shell nanowires. A, B) TEM images of the nanowires before and after the shell growth, C) powder XRD pattern of PbSe–PbS core–shell nanowires (NWRs), and D) HRTEM image of the core–shell nanowire.

the shell. TEM images of the PbSe wires before and after coating with a PbS shell are given in Figures 2A and B, respectively. Confirmation of the structure was obtained from the XRD pattern of the core–shell sample shown in Figure 3C. A shift of the diffraction peaks to higher angles

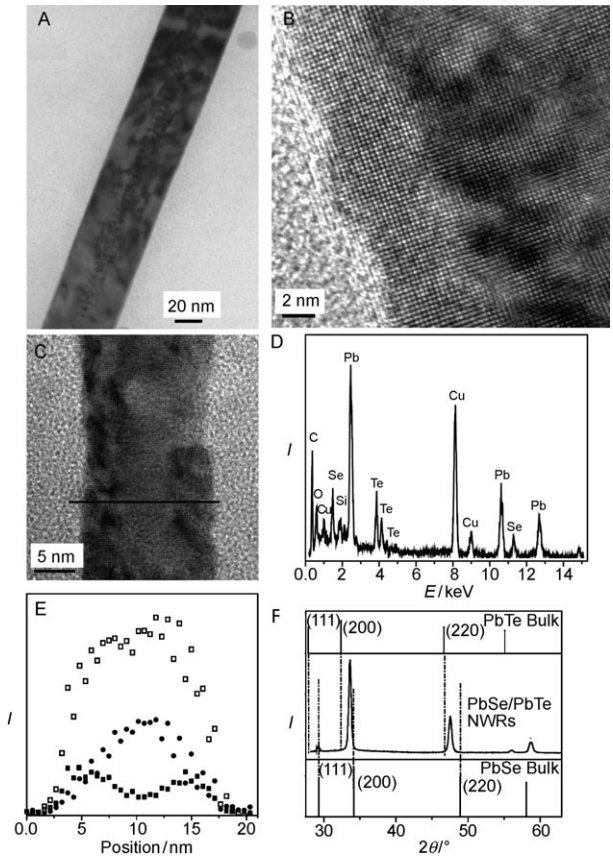

Figure 3. A) TEM image of a single PbSe–PbTe core–shell nanowire, B) HRTEM image of a PbSe–PbTe core–shell nanowire with a thin shell, C) TEM image of the same wire as that shown in (B). The black line indicates the path of the EDX line-scan. D) SA-EDX from the same area that the line-scan was performed, E) The line-scan spectrum (Pb □, Se ●, Te ■), and F) X-ray diffraction of the PbSe–PbTe core–shell nanowires with the PbSe and PbTe bulk diffraction patterns shown.

is observed as a result of the PbS shell growth. Such a shift is expected qualitatively due to the smaller lattice constant of the PbS (bulk pattern represented by the upper stick-spectrum) relative to the PbSe. This kind of effect was both experimentally observed and simulated for spherical core–shell particles.[17] The XRD measurement was carried out after purification of the sample through size-selective precipitation.

Further characterization of the PbSe–PbS core–shell structure was performed by HRTEM. The image in Figure 2D highlights a section of a PbSe–PbS core–shell nanowire. The structure appears to be single crystalline without observable defects at the interface, indicating an epitaxial relationship between the PbSe core and PbS shell. The observed 3 Å lattice spacing is in agreement with the (200) planes of the PbSe nanowires.

Similarly, the synthesis of PbSe–PbTe core–shell materials was achieved by a two-step synthesis, where the PbSe nanowires were prepared first and the shell was grown in the second stage. The shell thickness could be controlled nicely by changing the concentrations of the Pb and Te precursors. Control over the shell thickness is important for studying the influence of the shell on the physical and optical properties of the PbSe core. We achieved PbTe shell thicknesses ranging from 3 to 30 nm. The TEM image in Figure 3A shows a PbSe/PbTe core shell nanowire. The diameter of the PbSe nanowire before coating was ca. 8 nm and increased to 40 nm after PbTe deposition. A HRTEM image of a PbSe–PbTe core–shell nanowire with a thinner shell for visibility of the interface is presented in Figure 3B. The atomic resolution of the image allows for clear distinction between the core and the shell material. Careful examination of the interface between the core and the shell shows epitaxial growth, with the lattice mismatch between the PbSe and PbTe being only ca. 5.5% (6.126 and 6.462 Å, respectively).

Coating of a PbTe shell on the PbSe nanowires is carried out at a higher temperature compared to the PbS shell. Higher temperatures were required to grow a uniform epitaxial shell over the PbSe core because at lower temperatures free PbTe nanoparticles are formed and no shell growth is obtained. We prevented the homogeneous nucleation of stable PbTe nanocrystals, which are also formed at the temperature of shell growth, by adding the precursors slowly and in low concentration. Another challenge is to prevent formation of nonconformal core–shell structures and the development of small clusters/particles on the surface of the wires. These problems were minimized by annealing the wires in solution for 7 min at 130 °C, thereby allowing the formation of a uniform single-crystalline shell.

Further characterization of the PbSe–PbTe core–shell nanowires is shown in Figures 3C–F. Examination of the size of the nanowire in Figure 3C reveals that the shell thickness is 5 nm and the core is ca. 10 nm. An EDX spectrum on the area of the PbSe–PbTe core–shell nanowire shown in Figure 3C is provided in Figure 3D, indicating the presence of Pb, Se, and Te from the wire, and Cu from the TEM grid. Spatial resolution of the core–shell composition was determined by performing an EDX scan across the diameter of the nanowire. The line-scan was correlated with the physical position of the nanowire as denoted by the bold line in Figure 3C. The scan of signal intensity of Pb, Se, and Te along the cross section of the nanowire is plotted in Figure 3E. The Pb spectrum is spread along the cross section, which is expected due the existence of Pb in both the core and the shell. The Se signal starts to appear after 5 nm at the start of the core, and reaches a maximum at the center of the nanowire before decreasing again 5 nm before the end of the scan where the core terminates. The Te signal peaks at both edges of the wire in the shell zone, and decreases in the core area due to the cylindrical shape of the nanowire and the uniform shell coating.

The XRD pattern shown in Figure 3F of the PbSe–PbTe core–shell nanowires indicates a small shift to lower angles. The shift to lower angles is seen as result of the higher lattice

constant PbTe shell, in contrast to the shift to higher angles for the PbSe–PbS core–shell nanowires.

Lead chalcogenide heterostructures, including alloy and core–shell nanowires were achieved by solution phase synthesis using different synthetic approaches depending on the desired structure. These new heterostructures have a potential to provide better thermoelectric materials compared to the pure PbSe nanowires.

Experimental Section

Amorphous selenium shot (Aldrich, 99.999%), amorphous tellurium powder (Aldrich, 99.999%), sulfur powder (99.999%), lead acetate trihydrate (Fisher Scientific Co.), tri-*n*-octylphosphine (TOP) (Aldrich, 90%), and *n*-tetradecylphosphonic acid (TDPA) (Alfa, 97%) were used as purchased without further purification. Anhydrous tetrachloroethylene, diphenyl ether (DPE), and oleic acid were purchased from Aldrich. All syntheses were performed under Ar using a Schlenk line.

Synthesis of PbSe nanowires: The synthesis is based on a previous report.[16,18] Lead acetate trihydrate (0.76 g) and 2 mL of oleic acid were dissolved in 10 mL of diphenyl ether. The solution was heated to 150 °C for at least 30 min under Ar to form a lead–oleate complex. After 30–40 min the solution was cooled to 60 °C and mixed with the Se solution (4 mL of 0.167 M TOPSe solution in TOP). The Se solution was added slowly to prevent PbSe nucleation. The resulting PbSe solution was injected under vigorous stirring into a hot (250 °C) growth solution containing 0.2 g of TDPA dissolved in 15 mL of DPE (the growth solution was purified by heating to 180 °C). After 50 s of heating, the reaction mixture was cooled to room temperature using a water bath. The crude solution was mixed with an equal volume of hexane, and the nanowires were isolated by centrifugation at 6000 rpm for 5 min. The product (precipitate) was redispersed in chloroform or toluene for further characterization.

Synthesis of $PbSe_xS_{1-x}$ nanowires: A solution of S was prepared by dissolving 0.1 g of S in 0.5 mL of TOP and heating to 50 °C for 10 min before cooling to room temperature. The lead oleate solution was prepared using 0.2 g of lead acetate trihydrate, 2 mL of TOP, 2 mL of DPE, and 1.5 mL of oleic acid. The solution was heated to 150 °C for 30 min and then cooled to room temperature. At room temperature the S solution was added to the Pb solution with stirring. Simultaneously, 2 mL of DPE and 2 mL TOP were heated to 180 °C for 20–25 min and then cooled to room temperature before 30 mg of PbSe nanowires was added. This solution was reheated to 190–200 °C, and then the PbS solution was added dropwise (0.25 mL min^{-1}) to prevent self-nucleation. After the last addition, the solution was annealed for 10 min and then cooled to room temperature. The product was separated by adding hexane and centrifuging (6000 rpm) for 5 min.

Synthesis of PbSe–PbS core–shell nanowires: The shell synthesis was based on the successive ion layer adsorption and reaction (SILAR)[19,20] approach. The synthesis was carried out by slowly adding 0.3 mL of Pb (the same solution as that used for the alloy) and 0.1 mL of S solution (0.063 g, 2 mL TOP) to a growth solution, starting with Pb and then following with S after 3 min at a rate of 0.3 mL min^{-1}. The growth of the shell occurred at 130 °C, which is lower than the temperature for alloy formation. The growth solution contained 2 mL of DPE and 2 mL of TOP and was purified by heating to 200 °C for 25 min. After the solution had been cooled to room temperature, 30 mg of solid PbSe nanowires were added and the solution was reheated to 130 °C.

Synthesis of PbSe–PbTe core–shell nanowires: The growth of the shell was carried out by addition of 0.07 mg of Pb (the same solution as that used for the alloy) and 0.063 g of Te in 2 mL TOP. The Pb solution was dried by heating to 140 °C for 10 min, and after cooling to room temperature, the Te solution was added dropwise. This PbTe solution was then slowly added to the growth solution (at 190 °C), which contained 2 mL of TOP, 2 mL of DPE, and 20 mg of PbSe nanowires. After all of the precursors had been added, the reaction mixture was annealed at high temperature (130 °C) for another 7 min before cooling to room temperature. To separate the product, 2 mL of toluene and 2 mL of ethanol were added to the solution, which was then centrifuged for 5 min.

The structure and composition of the alloy and core–shell nanowires were investigated by transmission electron microscopy (TEM) (Technai 12) at 100 kV, high-resolution TEM (HRTEM) (Philips, CM200) at 200 kV, energy-dispersive X-ray spectroscopy (EDX) and electron energy loss spectroscopy (EELS). The X-ray diffraction (XRD) patterns were taken using $Co_{K\alpha}$ radiation (1.790 Å) and a general area detector (GADDS, Bruker). Samples were prepared by depositing a precipitated powder onto a quartz plate.

Received: March 10, 2008
Published online: June 13, 2008

Keywords: alloys · core–shell structures · lead chalcogenides · nanowires · thermoelectrics

[1] R. S. Wagner, W. C. Ellis, *Appl. Phys. Lett.* **1964**, *4*, 89 – 90.
[2] M. Law, J. Goldberg, P. Yang, *Annu. Rev. Mater. Res.* **2004**, *34*, 83 – 122.
[3] T. J. Trentler, K. M. Hickman, S. Goel, A. M. Viano, P. C. Gibbons, E. Buhro, *Science* **1995**, *270*, 1791 – 1794.
[4] J. Johnson, H. J. Choi, K. P. Knutsen, R. D. Schaller, P. Yang, R. J. Saykally, *Nat. Mater.* **2002**, *1*, 101 – 105.
[5] D. J. Sirbuly, A. R. Tao, M. Law, R. Fan, P. Yang, *Adv. Mater.* **2007**, *19*, 66 – 71.
[6] L. E. Brus, *J. Chem. Phys.* **1984**, *80*, 4403 – 4409.
[7] A. J. E. Nozik, *Inorg. Chem.* **2005**, *44*, 6893 – 6899.
[8] R. J. Ellingson, M. C. Beard, J. C. Johnson, P. Yu, O. I. Micic, A. J. Nozik, A. Shabaev, A. L. Efros, *Nano Lett.* **2005**, *5*, 865 – 871.
[9] R. D. Schaller, V. I. Klimov, *Phys. Rev. Lett.* **2004**, *92*, 186601.
[10] T. Mokari, U. Banin, *Chem. Mater.* **2003**, *15*, 3955 – 3960.
[11] E. Lifshitz, M. Brumer, A. Kigel, A. Sashchiuk, M. Bashouti, M. Sirota, E. Galun, Z. Burshtein, A. Q. Le Quang, I. Ledoux-Rak, J. Zyss, *J. Phys. Chem. B* **2006**, *110*, 25356 – 25365.
[12] M. Brumer, A. Kigel, L. Amirav, A. Sashchiuk, O. Solomesch, N. Tessler, E. Lifshitz, *Adv. Funct. Mater.* **2005**, *15*, 1111 – 1116.
[13] D. V. Talapin, H. Yu, E. V. Shevchenko, A. Lobo, C. B. Murray, *J. Phys. Chem. C* **2007**, *111*, 14049 – 14054.
[14] A. C. Bartnik, F. W. Wise, A. Kigel, E. Lifshitz, *Phys. Rev. B* **2007**, *75*, 245424.
[15] S. H. Wei, A. Zunger, *Phys. Rev. B* **1997**, *55*, 13605 – 13610.
[16] K. S. Cho, D. V. Talapin, W. Gaschler, C. B. Murray, *J. Am. Chem. Soc.* **2005**, *127*, 7140 – 7147.
[17] Y. W. Cao, U. Banin, *J. Am. Chem. Soc.* **2000**, *122*, 9692 – 9702.
[18] W. Lu, P. Gao, W. B. Jian, Z. Wang, J. Fang, *J. Am. Chem. Soc.* **2004**, *126*, 14816 – 14821.
[19] J. J. Li, Y. A. Wang, W. Guo, J. C. Keay, T. D. Mishima, M. B. Johnson, X. Peng, *J. Am. Chem. Soc.* **2003**, *125*, 12567 – 12575.
[20] A. Aharoni, T. Mokari, I. Popov, U. Banin, *J. Am. Chem. Soc.* **2006**, *128*, 257 – 264.

